

Ionospheric Alfv6n resonator revisited' Feedback instability I V. Khruschev i •/[. Parrot 2 S. Senchenkov, 1

Oleg A Pokhotelov, V. Khruschev, Michel Parrot, S. Senchenkov, V P Pavlenko

▶ **To cite this version:**

Oleg A Pokhotelov, V. Khruschev, Michel Parrot, S. Senchenkov, V P Pavlenko. Ionospheric Alfv6n resonator revisited' Feedback instability I V. Khruschev i •/[. Parrot 2 S. Senchenkov, 1. Journal of Geophysical Research Space Physics, 2001, 106, pp.25813-25824. insu-03234728

HAL Id: insu-03234728
https://insu.hal.science/insu-03234728

Submitted on 25 May 2021

HAL is a multi-disciplinary open access archive for the deposit and dissemination of scientific research documents, whether they are published or not. The documents may come from teaching and research institutions in France or abroad, or from public or private research centers.

L'archive ouverte pluridisciplinaire **HAL**, est destinée au dépôt et à la diffusion de documents scientifiques de niveau recherche, publiés ou non, émanant des établissements d'enseignement et de recherche français ou étrangers, des laboratoires publics ou privés.

JOURNAL OF GEOPHYSICAL RESEARCH, VOL. 106, NO. A11, PAGES 25,813–25,824, NOVEMBER 1, 2001

Ionospheric Alfvén resonator revisited: Feedback instability

Oleg A. Pokhotelov,[1] V. Khruschev,[1] M. Parrot,[2] S. Senchenkov,[1] and V. P. Pavlenko[3]

Abstract. The theory of ionospheric Alfvén resonator (IAR) and IAR feedback instability is reconsidered. Using a simplified model of the topside ionosphere, we have reanalyzed the physical properties of the IAR interaction with magnetospheric convective flow. It is found that in the absence of the convective flow the IAR eigenmodes exhibit a strong damping due to the leakage of the wave energy through the resonator upper wall and Joule dissipation in the conductive ionosphere. It is found that maximum of the dissipation rate appears when the ionospheric conductivity approaches the "IAR wave conductivity" and becomes infinite. However, the presence of Hall dispersion, associated with the coupling of Alfvén wave modes with the compressional perturbations, reduces the infinite damping of the IAR eigenmodes in this region and makes it dependent on the wavelength. The increase in the convection electric field leads to a substantial modification of the IAR eigenmode frequencies and to reduction of the eigenmode damping rates. For a given perpendicular wavelength the position of maximum damping rate shifts to the region with lower ionospheric conductivity. When the convection electric field approaches a certain critical value, the resonator becomes unstable. This results in the IAR feedback instability. A new type of the IAR feedback instability with the lowest threshold value of convection velocity is found. The physical mechanism of this instability is similar to the Čerenkov radiation in collisionless plasmas. The favorable conditions for the instability onset are realized when the ionospheric conductivity is low, i.e., for the nighttime conditions. We found that the lowest value of the marginal electric field which is capable to trigger the feedback instability turns out to be nearly twice smaller than that predicted by the previous analysis. This effect may result in the decrease of the critical value of the electric field of the magnetospheric convection that is necessary for the formation of the turbulent Alfvén boundary layer and appearance of the anomalous conductivity in the IAR region.

1. Introduction

The ionospheric Alfvén resonator (IAR) has been identified in the ground-based observations both in middle [*Polyakov and Rapoport*, 1981; *Belyaev et al.*, 1987, 1990] and in high latitudes [*Belyaev et al.*, 1999]. The analysis of Freja satellite data [e.g., *Grzesiak*, 2000] also confirms the existence of this phenomenon in the topside ionosphere. The IAR can be excited through a number of natural and manmade impacts. For example, it becomes unstable in the course of heating of the ionosphere by a powerful HF radio signal with a modulation frequency which lies in the range of IAR eigenfrequencies (0.1 – 10 Hz) [*Blagoveshchenskaya et al.*, 2001]. A comprehensive review of the artificial excitation of Alfvén waves in the IAR has been given recently by *Trakhtengertz et al.* [2000], who discussed two principal ways of such triggering. The first one assumes the use of two spaced transmitter antennas which produce an ionospheric current being in resonance with the IAR eigenmodes. The second method is based on the change in the macroscopic parameters of the ionosphere, such as conductivity in this region. The mechanism for the nonlinear excitation of the IAR by elves- and/or sprites-produced lightning discharges has been discussed by *Sukhorukov and Stubbe* [1997], who suggested that the anomalously large ULF transients observed in the upper ionosphere on board the satellites above strong at-

[1]Institute of Physics of the Earth, Moscow, Russia
[2] Laboratoire de Physique et Chimie de l'Environnement, Centre National de la Recherche Scientifique, Orléans, France
[3]Department of Space and Plasma Physics, University of Uppsala, Uppsala, Sweden.

Copyright 2001 by the American Geophysical Union.

Paper number 2000JA000450.
0148-0227/01/2000JA000450$09.00

mospheric weather systems [*Fraser-Smith*, 1993] are explained by excitation of the IAR eigenoscillations.

A basic mechanism of the IAR excitation in high latitudes is connected with the resonant interaction of the magnetospheric convective flow with the conductive ionosphere. If the convective flow is properly phased with the ionosphere and the magnetosphere, part of the energy of the convective flow is transferred to the IAR eigenmodes. This effect is known as the feedback instability, and it has been extensively studied by *Lysak* [1986, 1988, 1993, 1991, 1999] and *Trakhtengertz and Feldstein* [1981, 1984, 1987, 1991]. More general analysis of the IAR and the feedback instability has been provided recently by *Pokhotelov et al.* [2000]. In particular, the role of Hall divergent currents and, associated with them, Hall dispersion of the IAR eigenmodes, has been discussed. It was shown that the deceleration of the Alfvén wave phase velocity in the IAR due to Hall dispersion may increase the rate of energy transfer from the convective flow to the IAR eigenmodes and may overcome the dissipation rate due to Joule heating and the leakage of energy through the resonator upper boundary. The physical mechanisms of the feedback instability has much in common with the Čerenkov radiation in collisionless plasmas [*Pokhotelov et al.*, 2000].

It should be noted that the role of divergent Hall currents in magnetosphere-ionosphere coupling was recently emphasized by *Yoshikawa and Itonaga* [1996], and this effect was extensively studied by *Buchert and Budnik* [1997], *Yoshikawa et al.* [1999], and *Yoshikawa and Itonaga* [2000]. *Lysak* [1999] has recently performed numerical modeling of the magnetosphere-ionosphere system which also confirms the importance of Hall dispersion effects in the course of this interaction.

The physical reason for the IAR occurrence is due to a strong increase in Alfvén velocity with altitude, which results in violation of WKB approximation and subsequent wave reflection from velocity gradients. The latter leads to formation of a resonance cavity in the topside ionosphere. The analysis of the feedback instability provided by *Lysak* [1986, 1988, 1993, 1991], *Trakhtengertz and Feldstein* [1981, 1984, 1987, 1991], and *Pokhotelov et al.* [2000] was based on the assumption that Alfvén velocity in the ionosphere varies according to a simple analytical exospheric profile [*Greifinger and Greifinger*, 1968], which may be considered as representative. This makes it possible to express the IAR eigenfunctions in terms of Bessel functions and to obtain simple analytical expressions for the eigenfrequencies and the growth rates in two limiting cases of low and high ionospheric conductivity. However, in the most important case of finite ionospheric conductivity such an approach uses a quite complicated numerical analysis [e.g., *Lysak*, 1991] which does not often allow the drawing of a simple physical picture of the involved physical processes.

In this paper, using a simplified model for the Alfvén velocity profile, we will extend the previous analysis of the IAR and the feedback instability for arbitrary values of the ionospheric conductivity. We will analyze the properties of the IAR when it is disturbed by presence of convective flow. In addition to the earlier studies we will show that most favorable conditions for the IAR feedback instability are realized at low but finite ionospheric conductivity. We will find a new IAR instability which may arise at the value of the convection electric field that is smaller than predicted earlier.

The paper is organized as follows: section 2 is devoted to the derivation of a general dispersion relation for the IAR eigenmodes. The analysis of the IAR in the absence of the convective flow is given in section 3. The analysis of the IAR feedback instability is presented in section 4. Our discussions and conclusions are found in section 5.

2. IAR Dispersion Relation

In order to make our consideration as transparent as possible we consider a simplified model of a three-layer ionosphere shown in Figure 1. This model treats the ionosphere as a height-integrated slab, neglecting Hall and Pedersen conductivities above the ionospheric height. A similar model has been used to calculate the propagation of Alfvén waves in inhomogeneous media by *Mallinckrodt and Carlson* [1978]. The ionosphere-atmosphere interaction in our model is described by the conductive slab with a two-dimensional tensor conductivity

$$\hat{\Sigma} = \begin{pmatrix} \Sigma_P & -\Sigma_H \\ \Sigma_H & \Sigma_P \end{pmatrix}, \tag{1}$$

where Σ_P and Σ_H correspond to height-integrated Pedersen and Hall conductivities, respectively. In such a model the IAR is localized in the homogeneous layer with the Alfvén velocity defined as $v_{AI} = B/(\mu_0 \rho_I)^{1/2}$, where B is the magnitude of the external magnetic field $\mathbf{B}$, μ_0 is the permeability of free space, and ρ_I is the IAR plasma mass density. The homogeneous layer above the IAR with plasma density $\rho_M \ll \rho_I$ represents the magnetosphere. We assume also that in the unperturbed state, there is a convective flow moving with the constant velocity $\mathbf{v}_0 = (\mathbf{E}_0 \times \hat{\mathbf{z}})/B$, where $\mathbf{E}_0$ is the electric field due to the magnetospheric convection and $\hat{\mathbf{z}}$ is a unit vector along $\mathbf{B}$. As we shall see in what follows, this simplified model qualitatively describes all basic features of the problem at hand. In addition, it allows us to reveal additional physical features of the IAR which have not been discussed earlier.

Let us consider all perturbed quantities to vary as $\exp(-i\omega t)$, where ω is the wave frequency. In the reference frame moving with the convection velocity $\mathbf{v}_0$, the shear Alfvén and compressional modes are described by a set of differential equations [cf. *Pokhotelov et al.*, 2000]

$$\partial_z^2 \Phi + \frac{\omega^2}{v_A^2(z)} \Phi = 0, \tag{2}$$

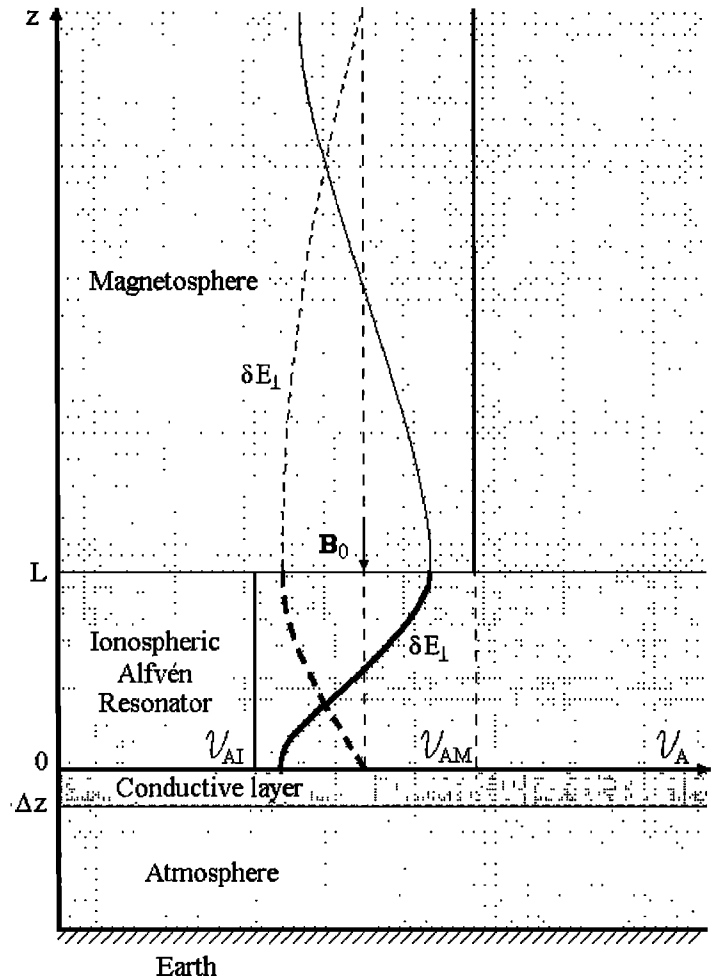


Figure 1. Schematic diagram of the IAR model. The variation of perpendicular electric field $\delta E_\perp$ with the altitude for the fundamental eigenmodes is shown. The case of low ionospheric conductivity is indicated by a solid curve, whereas the dashed curve corresponds to high conductivity.

$$\nabla^2\Psi + \frac{\omega^2}{v_A^2(z)}\Psi = 0, \tag{3}$$

where $v_A(z) = B/(\mu_0\rho)^{1/2}$ is the altitude-dependent Alfvén velocity, ρ is the plasma mass density, $\partial_z \equiv \partial/\partial z$, and $\nabla^2 = \partial_z^2 + \nabla_\perp^2$. The potentials Φ and Ψ are connected with the perturbed electric $\delta\mathbf{E}_\perp$ and magnetic $\delta\mathbf{B}_\perp$ fields by the following relations

$$\delta\mathbf{E}_\perp = -\nabla_\perp\Phi + i\omega\nabla_\perp \times \Psi\hat{\mathbf{z}}, \tag{4}$$

$$\delta\mathbf{B}_\perp = \nabla_\perp A \times \hat{\mathbf{z}} + \nabla_\perp\partial_z\Psi, \tag{5}$$

$$\delta\mathbf{B}_z = -\nabla_\perp^2\Psi. \tag{6}$$

Here the parallel component of the vector potential A and the scalar potential Φ are not independent because we consider that the field-aligned electric field in our plasma is zero; that is, $E_z = -\partial_z\Phi + i\omega A = 0$. Such an assumption is justified if the wavelengths of the considered perturbations are much larger than the collisionless electron skin depth.

The solution of equation (2) in the internal region (IAR region) has the form of a superposition of downgoing and upgoing waves

$$\Phi = A_1 \exp(iz\omega/v_{\mathrm{AI}}) + A_2 \exp(-iz\omega/v_{\mathrm{AI}}). \tag{7}$$

In the external region (magnetosphere) we assume that only the outgoing wave remains, that is,

$$\Phi = C\exp(i\varepsilon z\omega/v_{\mathrm{AI}}), \tag{8}$$

where $\varepsilon = v_{\mathrm{AI}}/v_{\mathrm{AM}} \ll 1$ is the ratio of the Alfvén velocities in the IAR and in the magnetosphere and A_1, A_2, and C are constant values.

According to *Trakhtengertz and Feldstein* [1991], such an approximation corresponds to the so-called radiation condition at infinity. The necessary matching of solutions (7) and (8) at the upper IAR boundary, that is, at $z = L$, requires the continuity of both the potential and its first derivative. The necessary matching at the

upper IAR wall gives

$$A_2 = A_1(1-2\varepsilon)\exp(2ix_0), \tag{9}$$

$$C = 2A_1(1-\varepsilon)\exp[i(1-\varepsilon)x_0], \tag{10}$$

where $x_0 = \omega L/v_{\rm AI}$. The terms of the order of ε^2 in (9) and (10) are neglected.

We consider the perpendicular wavelength to be much smaller than both $v_{\rm AI}/\omega$ and $v_{\rm AM}/\omega$. Replacing $\nabla_\perp^2$ by $-k_\perp^2$ (where $k_\perp$ is the perpendicular wave number) in equation (3), we find that the compressional component of the magnetic field, described by the potential Ψ, decays as $\propto \exp(-k_\perp z)$ in both regions, that is,

$$\Psi = \Psi_0 \exp(-k_\perp z) \qquad 0 < z < \infty, \tag{11}$$

where Ψ_0 is a constant value.

These equations should be supplemented by two boundary conditions on the conductive slab ($z = 0$). The ionosphere-atmosphere interaction is controlled by the height-integrated current flowing in the lower ionosphere. In our reference frame the conductive slab moves with the velocity $-\mathbf{v}_0$. Thus Ohm's law, integrated across the slab, can be written as [cf. *Pokhotelov et al.*, 2000]

$$\delta\mathbf{J}_\perp = \Sigma_P\delta\mathbf{E}_\perp + \Sigma_H\hat{\mathbf{z}}\times\delta\mathbf{E}_\perp - B[\Sigma_P(\mathbf{v}_0\times\hat{\mathbf{z}}) + \Sigma_H\mathbf{v}_0]\frac{\delta n}{n}, \tag{12}$$

where $\delta\mathbf{J}_\perp$ denotes the change in the perpendicular height-integrated electric current and δn is the perturbation of the ionospheric density which arises in the ionosphere due to the particle precipitation and recombination processes. Hall and Pedersen conductivities are assumed to be uniform, and their perturbed values $\delta\Sigma_P$ and $\delta\Sigma_H$ are considered to scale as $\propto \delta n$. This is a reasonable approach as long as the ionospheric temperature and the neutral density do not vary significantly because of the field-aligned currents or subsequent particle precipitation [*Lysak*, 1991]. Expression (12) shows that the presence of the convective flow may substantially modify the ionospheric current and can significantly change the properties of the IAR.

We assume that the field-aligned current does not penetrate into the insulated atmosphere; that is, the condition $j_{||}(-\Delta z) = 0$ is satisfied. According to Ampère's law the latter means that divergence of $\delta\mathbf{J}_\perp$ produces only the ionospheric field-aligned current, and thus we have $i\mathbf{k}_\perp\cdot\delta\mathbf{J}_\perp = -j_{||}$ on the upper boundary of the conductive slab. With the help of the parallel component of Ampère's law this condition reduces to

$$\mathbf{k}_\perp\cdot\delta\mathbf{J}_\perp = \frac{k_\perp^2\Sigma_w v_{\rm AI}}{\omega}\partial_z\Phi, \tag{13}$$

where $\Sigma_w = 1/\mu_0 v_{\rm AI}$ is the "IAR wave conductivity."

Dotting $\delta\mathbf{J}_\perp$, given by (12), with $\mathbf{k}_\perp$ and using (13), gives

$$(v_{\rm AI}/\omega)\partial_z\Phi + i\alpha_P\Phi + \omega\alpha_H\Psi + Bk_\perp^{-2}[\alpha_P(\mathbf{k}_\perp\times\mathbf{v}_0)_z + \alpha_H(\mathbf{k}_\perp\cdot\mathbf{v}_0)]\frac{\delta n}{n} = 0. \tag{14}$$

Here $\alpha_P = \Sigma_P/\Sigma_w$ and $\alpha_H = \Sigma_H/\Sigma_w$ are dimensionless Pedersen and Hall conductivities, respectively. Usually, in the ionosphere they are connected to each other. For example, for sunlight-produced conductivity, $\alpha_H \simeq 2\alpha_P$, whereas for precipitation-produced conductivity, $\alpha_H/\alpha_P \simeq E^{5/8}$, where E is the energy of precipitating electrons in keV [e.g., *Spiro et al.*, 1982]. This ratio is 4.2 for 10 keV electrons and 2.7 for 5 keV. Large values of α_H/α_P of the order of 5 and higher may take place in the auroral zone (e.g., *Brekke et al.* [1974]; see also discussion provided by *Yoshikawa and Itonaga* [1996]).

The change in the ionospheric density is controlled by the continuity equation, which in our reference frame takes the form [*Lysak*, 1991]

$$-i\omega\delta n + i\mathbf{k}_\perp\cdot(n\delta\mathbf{v}_E) = \gamma\left(\frac{j_{||}}{e\Delta z}\right) - \nu\delta n, \tag{15}$$

where $\delta\mathbf{v}_E = (\delta\mathbf{E}_\perp\times\hat{\mathbf{z}})/B$, e is the magnitude of the electronic charge, Δz is the depth of the conductive slab, γ represents the number of additional electron-ion pairs created per incident electron, and ν is an effective recombination frequency.

The solution of equation (15) gives

$$\frac{\delta n}{n} = \frac{k_\perp^2 B^{-1}[\alpha_I^{-1}(v_{\rm AI}/\omega)\partial_z\Phi + \omega\Psi]}{\omega + i\nu}. \tag{16}$$

Here $\alpha_I = (\Delta z/\lambda_{pi})\gamma^{-1}$ is the dimensionless parameter, which controls the electron precipitation, $\lambda_{pi} = c/\omega_{pi}$ is the collisionless ion skin depth, c is the speed of light, $\omega_{pi} = (ne^2/\varepsilon_0 m_i)^{1/2}$ is the ion plasma frequency, and m_i is the ion mass. For the actual ionospheric conditions, γ is nearly a linear function of the incoming electron energy. It is about 100 for 10 keV electrons [*Rothwell et al.*, 1984]. According to *Lysak* [1991] $\Delta z \simeq \lambda_{pi} \simeq 10-30$ km. Therefore α_I is a small parameter of the order of $10^{-1}-10^{-2}$. A typical recombination frequency for the ionospheric density of $n \simeq 10^{11}$ m^{-3} and recombination coefficient $R = \nu/2n \simeq 10^{-13}$ m^3 s^{-1} is $\nu \simeq 10^{-2}$ s^{-1}.

Combining (14) and (16), we obtain

$$(1-\frac{\Sigma_\varphi}{\omega+i\nu})\frac{v_{\rm AI}}{\omega}\partial_z\Phi + i\alpha_P\Phi + \omega\alpha_H(1-\frac{\alpha_I\alpha_H^{-1}\Sigma_\varphi}{\omega+i\nu})\Psi = 0, \tag{17}$$

where

$$\Sigma_\varphi = -\frac{k_\perp v_0\alpha_C}{\alpha_I}\cos[\varphi - \arctan(\alpha_P/\alpha_H)], \tag{18}$$

with

$$\alpha_C = (\alpha_P^2 + \alpha_H^2)^{1/2}.$$

If Ψ is properly expressed through Φ, equation (17), together with solutions (7)-(11), describes the dispersion relation for the IAR eigenfrequencies. The necessary connection can be obtained by applying $(\nabla\times)_z$ to Ampère's law, which gives [cf. *Pokhotelov et al.*, 2000]

$$(\partial_z^2 - k_\perp^2)\Psi = -i\mu_0 k_\perp^{-2}(\mathbf{k}_\perp \times \delta\mathbf{j}_\perp)_z, \qquad (19)$$

where $\delta\mathbf{j}_\perp$ is the change in the perpendicular ionospheric current.

Integration of (19) gives

$$\partial_z\Psi(0) - \partial_z\Psi(-\Delta z) - k_\perp^2\Delta z\Psi(0) = -i\mu_0 k_\perp^{-2}(\mathbf{k}_\perp\times\delta\mathbf{J}_\perp)_z \qquad (20)$$

On one hand, according to (11), Ψ falls off exponentially above the conductive slab, i.e., $\Psi \propto \exp(-k_\perp z)$. On the other hand, in the neutral atmosphere $(-d < z < \Delta z)$, Ψ varies as [e.g., *Yoshikawa and Itonaga*, 1996]

$$\Psi = C\frac{\exp(k_\perp z) - \exp[-k_\perp(z+2d)]}{1-\exp(-2k_\perp d)}, \qquad (21)$$

where C is a constant value.

Expression (21) is valid if Ψ vanishes on the surface $z = -d$. Such simplification assumes that the solid Earth is considered to be a perfect conductor. In reality, magnetometer chains above the solid ground do register large-scale variations of external origin in Ψ, suggesting that $\Psi \neq 0$ [*Buchert and Budnik*, 1997]. Thus, strictly speaking, our assumption of a conducting Earth is satisfied above the sea and close to it. Otherwise, the effects due to the finite Earth's conductivity should be taken into consideration, and (21) should be replaced by a more complex expression. Consideration of this effect is, however, out of the scope of the present paper. We note that the limit of nonconducting Earth was discussed by *Buchert and Budnik* [1997]. In the limiting case $k_\perp d \gg 1$ the compressional mode falls off as $\exp(-k_\perp \mid z \mid)$ on both sides of the ionospheric sheet [*Pokhotelov et al.*, 2000].

With the help of (21) we find

$$\partial_z\Psi(-\Delta z) = Ck_\perp\exp(-k_\perp\Delta z)\frac{1+\exp[2k_\perp(\Delta z - d)]}{1-\exp(-2k_\perp d)}$$

$$\simeq Ck_\perp\exp(-k_\perp\Delta z)\coth(k_\perp d), \qquad (22)$$

where we assumed that the depth of the conductive slab is much smaller than its altitude above the ground, i.e., $\Delta z \ll d$.

Using (11) and (22), we find

$$\Psi = \frac{i\mu_0 k_\perp^{-3}(\mathbf{k}_\perp\times\delta\mathbf{J}_\perp)_z}{\kappa k_\perp}, \qquad (23)$$

where $\kappa = 1 + k_\perp\Delta z + \exp(-k_\perp\Delta z)\coth(k_\perp d)$. With the help of (12) from (23) we finally obtain

$$\Psi[\kappa - \frac{i\alpha_P\omega}{k_\perp v_{AI}} - \frac{i\alpha_I\omega\Delta_\varphi}{k_\perp v_{AI}(\omega+i\nu)}] = \frac{\alpha_H}{k_\perp v_{AI}}\Phi$$

$$+\frac{i\Delta_\varphi}{k_\perp v_{AI}}\frac{v_{AI}}{\omega}\partial_z\Phi, \qquad (24)$$

where

$$\Delta_\varphi = -\frac{k_\perp v_0\alpha_C}{\alpha_I}\sin[\varphi - \arctan(\alpha_P/\alpha_H)]. \qquad (25)$$

Equations (17) and (24), together with (7)-(12), form a closed system of equations which describes the dispersion equation for the IAR eigenmodes in the presence of the convective flow. They generalize the corresponding equations of *Pokhotelov et al.* [2000] by inclusion of finite $k_\perp\Delta z$ and $k_\perp d$ effects. In a special case when $k_\perp d \ll 1$ (which also assumes $k_\perp\Delta z \ll 1$) we have $\kappa = (k_\perp d)^{-1} \gg 1$. This situation was analyzed by *Polyakov and Rapoport* [1981]. We note that since for the real conditions $d \simeq 10^2$ km, such an approximation is relevant only for the perpendicular wave lengths $\lambda_\perp \gg 2\pi d \simeq 600$ km. Such waves do not satisfy the Čerenkov resonant condition that is necessary for the IAR excitation by magnetospheric convective flow [e.g., *Pokhotelov et al.*, 2000], thus another limiting case for which $k_\perp d \gg 1$ seems to be more relevant for our study. Such waves are effectively trapped in the IAR and can accumulate a sufficient amount of energy to influence the aurora [*Trakhtengertz and Feldstein*, 1987]. In this limiting case $\coth(k_\perp d) \to 1$ and $\kappa \simeq 1 + k_\perp\Delta z + \exp(-k_\perp\Delta z)$. We note that the analysis of *Pokhotelov et al.* [2000] corresponds to the so-called zero-Δz approximation, when $k_\perp\Delta z \leq 1$ and $\kappa = 2$. Since for the real ionospheric conditions Δz can be of the order of one tenth of a kilometer, another limiting case, when $k_\perp\Delta z \gg 1$ and $\kappa = k_\perp\Delta z$, may become more relevant for the interpretation of observations.

3. IAR in Absence of Convective Flow: Role of Hall Dispersion

Let us consider the case when the convection electric field vanishes, that is, $\mathbf{E}_0 = 0$. In addition, we neglect the corrections due to Hall dispersion. In this limiting case, equation (17) reduces to *Lysak* [1991] type

$$(v_{AI}/\omega)\partial_z\Phi + i\alpha_P\Phi = 0, \qquad (26)$$

Substitution of (7)-(10) into (26) gives

$$\exp 2ix_0 = (1+2\varepsilon)\frac{1+\alpha_P}{1-\alpha_P}. \qquad (27)$$

Decomposing the dimensionless frequency in equation (27) into the real and imaginary parts, $x_0 = \eta + i\gamma$, we get

$$\exp(2i\eta - 2\gamma) = (1+2\varepsilon)\left|\frac{1+\alpha_P}{1-\alpha_P}\right|\exp(i\vartheta_\alpha + 2ik\pi), \qquad (28)$$

where $\vartheta_\alpha = \arg[(1+\alpha_P)/(1-\alpha_P)]$ and k is integer, that is, $k = 0, 1, 2, \ldots$. From equation (28) we obtain

$$\gamma = -\varepsilon - \frac{1}{2}\ln\left|\frac{1+\alpha_P}{1-\alpha_P}\right|, \qquad (29)$$

$$\eta = k\pi \qquad 0 \le \alpha_P < 1, \qquad (30)$$

$$\eta = \frac{(2k+1)}{2}\pi \qquad 1 < \alpha_P < \infty, \qquad (31)$$

where, again, the small terms of the order of ε^2 are neglected.

The following comments are in order. The first term on the right in (29) describes the IAR damping due to the leakage of the wave energy through the resonator upper wall, whereas the second term corresponds to losses due to the ionosphere Joule heating. When $\alpha_P \to 1$, that is, when the ionosphere and the magnetosphere are optimally matched, the damping becomes infinite. Moreover, when $\alpha_P = 1$, the mode frequencies undergo a finite jump. We term the region with sharp frequency variation as a transition region [cf. *Yoshikawa et al.*, 1999]. It should be mentioned that here Hall dispersion, which has been neglected in equation (27), may play an essential role. We will return to this problem in the end of this section.

The plots of dimensional frequency and damping rate as a function of α_P are shown in Figure 2, using solid curves. Figure 2 shows that through the transition region, the kth harmonic for the insulator-like ionosphere is connected with the $(k+1)$th harmonic for the conductor-like ionosphere. One of the peculiar features of the IAR eigenmodes shown in Figure 2 (top) is related to the fact that the counterpart for the fundamental harmonic ($k = 0$) for the conductor-like ionosphere ($\alpha_P > 1$) corresponds to a zero-frequency mode in the insulator-like ionosphere ($\alpha_P < 1$). This variation of mode frequencies and the damping factor is similar to that discussed by *Newton et al.* [1978] and *Miura et al.* [1982] for the localized toroidal oscillation under the dipole magnetic field model. Recently, *Yoshikawa et al.* [1999] provided a physical interpretation for this connection. According to this paper the existence of interconnected harmonics arises from a type of conservation of parity in that the spatial structure of the eigenmode along the field line is either symmetric or antisymmetric in nature. Conservation of parity assumes the keeping of a symmetric or antisymmetric nature of field line oscillation even when the geometrical changes of oscillation have occurred by the parametric change in ionospheric conductivity.

We note that the values of the eigenfrequencies, obtained in our model, are different from those obtained in a model with smooth exospheric profile of the Alfvén velocity [e.g., *Lysak*, 1991; *Trakhtengertz and Feldstein*, 1991]. We recall that in such a model, variation of the Alfvén velocity with the altitude is described by a simple expression [*Greifinger and Greifinger*, 1968]

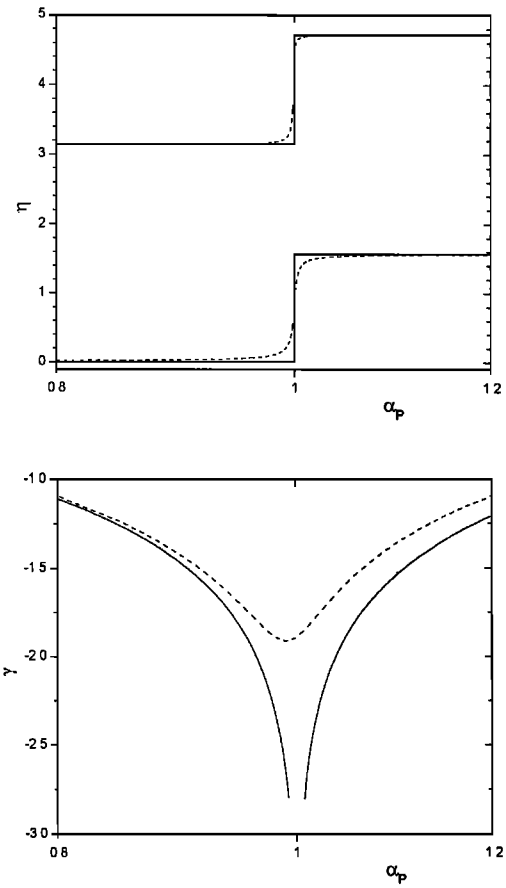


Figure 2. Variation of the frequency and the damping rate for the IAR eigenmodes as the function of α_P in the absence of convective flow ($\varepsilon = 0.01$, $\nu = 0.01$, $k_\perp d = 60$, $d = 100$ km, $\Delta z = 30$ km and $L = 1000$ km). (Top) Solid curve shows the variation of dimensionless eigenfrequency as a function of the dimensionless Pedersen conductivity in the absence of Hall dispersion. Dashed curve corresponds to the case when Hall dispersion effect is included ($\alpha_H = \alpha_P$). (Bottom) Same as top but for the damping rate.

$$v_A^2(z) = \frac{v_{AI}^2(z)}{\varepsilon^2 + \exp(-2z/L)}, \qquad (32)$$

where, as in our model, $\varepsilon \ll 1$ defines the ratio of the Alfvén velocity v_{AI} in the ionosphere to that in the outer magnetosphere v_{AM} so that $v_{AI}/v_{AM} \simeq \varepsilon$.

According to *Lysak* [1991] and *Trakhtengertz and Feldstein* [1991], for low ($\alpha_P \ll 1$) and high ($\alpha_P \gg 1$) ionospheric conductivity the IAR dimensionless eigenfrequencies are defined by the roots of the Bessel functions of the first and zero order, respectively. The first three roots of equation $J_1(\eta) = 0$ are 0, 3.8, and 7. They are close to 0, π, and 2π and describe the dimensionless eigenfrequencies of the IAR in our model in the low conductivity case. Similarly, for highly conductive ionosphere we have $J_0(\eta) = 0$, and the corresponding roots are 2.4 and 5.5 which are not essentially different from $\pi/2$ and $3\pi/2$. Thus our simplified model qualitatively describes basic physical properties of the IAR.

According to (29) the resonator undergoes a weak damping in the two limiting cases of low and high ionospheric conductivities. Making the corresponding expansion, from (29) we get

$$\gamma = -\varepsilon - \alpha_P \qquad \alpha_P \ll 1, \tag{33}$$

$$\gamma = -\varepsilon - 1/\alpha_P \qquad \alpha_P \gg 1. \tag{34}$$

If one neglects this damping, then the IAR eigenfunctions in these two limiting cases will take the form

$$\Phi = 2A_1[\cos(z\omega/v_{\rm AI}) - \varepsilon \exp(-iz\omega/v_{\rm AI})] \qquad \alpha_P \ll 1, \tag{35}$$

$$\Phi = 2iA_1[\sin(z\omega/v_{\rm AI}) - i\varepsilon \exp(-iz\omega/v_{\rm AI})] \qquad \alpha_P \gg 1, \tag{36}$$

which correspond to a superposition of a standing wave and a wave reflected from the upper boundary of the IAR wall. When $\alpha_P \ll 1$ and $\alpha_P \gg 1$, the resonator eigenmodes are as shown in Figure 1, with bold and bold dashed curves, respectively.

The inclusion of Hall dispersion removes a discontinuity in the variation of the IAR damping rate as well as the jump in the variation of eigenfrequency. Moreover, the presence of Hall dispersion replaces the zero-frequency mode by a finite-frequency mode. To demonstrate this, we generalize the dispersion equation for the IAR eigenfrequencies by considering this effect. Then equation (27) can be written as

$$\exp(2ix_0) = (1 + 2\varepsilon)\frac{1 + \tilde{\alpha}_P}{1 - \tilde{\alpha}_P}, \tag{37}$$

where

$$\tilde{\alpha}_P = \alpha_P - \frac{i\alpha_H^2 x_0}{\kappa k_\perp L(1 - i\alpha_P x_0/\kappa k_\perp L)}. \tag{38}$$

The contribution of the second term on the right into equation (37) is always small, except for the case when $\alpha_P \simeq 1$. The presence of this additional term will smooth the variation of the frequency and the damping rate in the transition region which now scales as $\propto \ln(\kappa k_\perp L)$ at $\alpha_P = 1$. This is shown in Figure 2 (upper and lower panels) by a dashed curve. It is worth mentioning that a similar effect of disappearance of singularity at $\alpha_P = 1$ due to Hall correction in the expression for the wave reflection coefficient can be revealed by *Polyakov and Rapoport* [1981] analysis (e.g., equation (11)). However, this expression was obtained in the limiting case $k_\perp d \ll 1$ when IAR eigenmodes do not effectively interact with the magnetospheric convective flow. Fine peculiarities of the change in mode frequency and damping rate become more clear if we make an expansion of equation (37) in two limiting cases of small and high ionospheric conductivities. For low ionospheric conductivity ($\alpha_P \ll 1$) from (37) we obtain $\eta = 0$ for $k = 0$ and $\eta = \pi(1 - \alpha_H^2/\kappa k_\perp L)$ for $k = 1$.

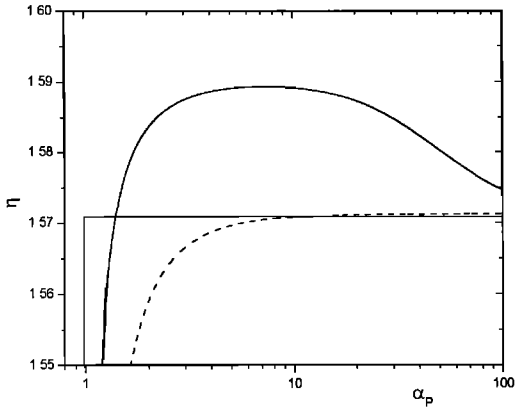


Figure 3. Variation of the dimensionless mode frequency in the vicinity of $\eta \simeq \pi/2$ for different values of α_H/α_P. Solid curve corresponds to $\alpha_H/\alpha_P = 12$, dashed curve corresponds to $\alpha_H/\alpha_P = 1.75$. Other parameters are the same as in Figure 2.

This agrees with *Pokhotelov et al.* [2000], who demonstrated that the IAR eigenfrequency at $k = 1$ undergoes a red frequency shift induced by Hall dispersion. The zero-frequency solution is not influenced by Hall dispersion in this approximation, whereas the damping rate becomes smaller $\gamma = -(\varepsilon + \alpha_P)/(1 + \alpha_H^2/\kappa k_\perp L)$. In the opposite limiting case, $\alpha_P \gg 1$, the corresponding expansion of equation (37) for the lowest mode ($k = 1$) gives $\eta = \pi/2 + 2\alpha_H^2 \kappa k_\perp L/\pi(\alpha_P^2 + \alpha_H^2)^2$ and $\gamma = -\varepsilon - \alpha_P/(\alpha_P^2 + \alpha_H^2)$. Thus the mode frequency exhibits a blue frequency shift due to Hall dispersion, and the damping rate is substantially modified by the presence of Hall conductivity. The latter is connected with fact that a divergent Hall current becomes large for high conducting ionosphere, and the divergent Pedersen current is shielded [cf. *Yoshikawa and Itonaga,* 2000]. The change in fundamental mode frequency for the finite values of α_P and different ratios of α_H/α_P is shown in Figure 3. One can see that Hall effects lead to the appearance of a maximum in the variation of the mode frequency. A similar effect was reported by *Yoshikawa and Itonaga* [1996] in the course of the analysis of wave reflection at the ionosphere. Since they have analyzed much longer wavelengths, this maximum is more pronounced in their study than in our case, when Hall corrections are small.

It is worth mentioning that rigorous consideration of the limiting case of perfectly conducting ionosphere ($\alpha_P \gg 1$) requires a special consideration which is out of the scope of the present study. We note that since the IAR eigenperiods are usually smaller than several seconds, the approximation of the thin sheet conductive layer may not be satisfied in this limit. The validity of this approximation requires that the depth of conductive layer Δz must be smaller than the skin depth $\lambda_s = (2/\mu_0\omega_m\sigma_P)^{1/2}$, where σ_P stands for Pedersen conductivity and ω_m is the IAR eigenfrequency. This inequality can be rewritten as $\Delta z \ll (2\Delta z L/\eta_m\alpha_P)^{1/2}$ or $\Delta z \ll 2L/\eta_m\alpha_P$ (here $\eta_m = \omega_m L/v_{\rm AI}$, for the fun-

damental mode $\eta_m \simeq \pi/2$). It is evident from this estimation that the thin sheet approximation, adopted in our analysis, may be violated in the conductor-like ionosphere for very large values of α_P.

4. IAR Modification Induced by Convective Flow: Feedback Instability

Let us now consider how the presence of convective flow modifies the physical properties of the IAR eigenmodes. For this aim, equations (17) and (24) have been solved numerically. As an example, the change in the dimensionless frequency of the lowest (fundamental) IAR eigenfrequency for different values of $\sigma = \sigma_{\varphi\max}$ is shown in Figure 4. Here $\sigma_{\varphi\max} \equiv \Sigma_{\varphi\max} L/v_{\rm AI}$ and $\varphi = \varphi_{\max}$ stands for the angle of propagation, calculated numerically, which yields the maximum value of growth/damping rate. It is clearly seen that with the increase in the convection electric field the major modification of the mode appears basically at $\alpha_P < 1$, that is, when the ionospheric conductivity is low. The modification results in two effects. On one hand, the transition region shifts toward the lower ionospheric conductivity. On the other hand, the fundamental eigenmode frequency increases in value. The damping of the IAR mode becomes weaker. Figure 5 shows the change in the damping rate of the fundamental mode. With the increase in the convection electric field the maximum value of the damping rate decreases and the position of a minimum shifts to the lower conductivity. Eventually, the growth rate becomes positive when $\sigma > \pi/2$. The condition $\sigma \simeq \pi/2$ corresponds to the marginal stability of our system. In this limiting case equations (17) and (24) possess an analytical solution. We note that for marginal stability, $\sigma \simeq \pi/2$, the value of $\delta_\varphi \equiv \Delta_{\varphi\max} L/v_{\rm AI}$ vanishes, $\delta_\varphi \simeq 0$, and thus the corresponding terms in equation (17) are small [*Pokhotelov et al.*, 2000]. Taking into account these considerations, from (17) we obtain

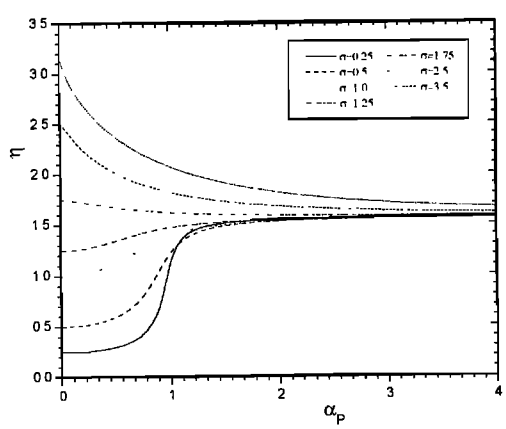


Figure 4. Variation of the IAR fundamental eigenfrequency as the function of α_P for different values of σ. Here $\alpha_H/\alpha_P = 1.75$. Other parameters are the same as in Figure 2.

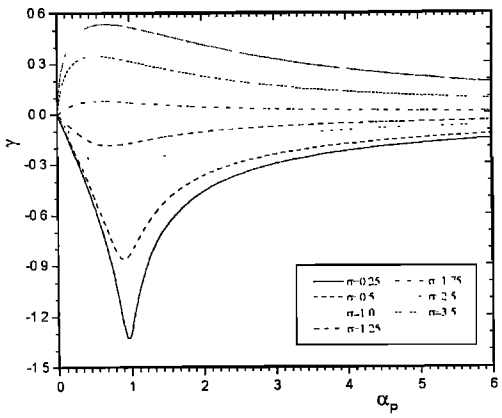


Figure 5. Same as Figure 4 but for the damping/growth rate.

$$\alpha_P + \left(1 - \frac{\sigma_\varphi}{x_0 + i\nu}\right) \frac{1 - (1-2\varepsilon)e^{2ix_0}}{1 + (1-2\varepsilon)e^{2ix_0}}$$

$$- \frac{i\alpha_H^2 x_0}{\kappa k_\perp L}\left(1 - \frac{\alpha_I \alpha_H^{-1} \sigma_\varphi}{x_0 + i\nu}\right) = 0, \qquad (39)$$

where, contrary to section 2, the recombination frequency ν is dimensionless, that is normalized to $v_{\rm AI}/L$.

Equation (39) can be further simplified. Similar to *Pokhotelov et al.* [2000], it can be shown that the last term on the left, which describes the corrections due to Hall dispersion, leads to a small increase in the wave growth rate. Neglecting this effect, we finally obtain

$$\alpha_P + \left(1 - \frac{\sigma_\varphi}{x_0 + i\nu}\right)\left(\frac{1 - (1-2\varepsilon)e^{2ix_0}}{1 + (1-2\varepsilon)e^{2ix_0}}\right) = 0. \qquad (40)$$

Let us search for the solution of (40) near the lowest IAR resonance, that is, in the vicinity of the solution of equation $1 + (1-2\varepsilon)e^{2ix_0} = 0$. The latter equation has the lowest weakly damping root $x_0 = x_0^* = \pi/2 - i\varepsilon$. Introducing $\Delta x_0 = x_0 - x_0^*$, from (40) we obtain

$$(x_0 - x_0^*)(1 - i\alpha_P x_0^* + \nu\alpha_P) - (\sigma_\varphi - x_0^*) + i\nu = 0. \qquad (41)$$

When splitting x_0 into real and imaginary parts, we find for the respective dimensionless frequency and growth rate

$$\eta = \sigma_\varphi - \frac{\pi\alpha_P}{2}(\varepsilon - \nu), \qquad (42)$$

$$\gamma = -\nu + \frac{\pi\alpha_P}{2}(\sigma_\varphi - \frac{\pi}{2}). \qquad (43)$$

From the first term on the right in (43) one immediately recognizes the damping due to recombination processes. We note that the damping due to the energy leakage through the upper IAR wall is exactly counterbalanced by the effect of accumulation of energy in the resonator due to the wave reflection from the IAR upper boundary.

Using (18) we find that instability ($\gamma \geq 0$) arises for the angles of propagation

$$\cos(\varphi - \arctan\frac{\alpha_P}{\alpha_H}) \leq -\frac{v^{cr}}{v_0}, \tag{44}$$

with

$$v^{cr} = \frac{\alpha_I v_{AI}\pi}{2k_\perp L\alpha_C}\left[1+\frac{\nu}{\alpha_P}\left(\frac{2}{\pi}\right)^2\right]. \tag{45}$$

Such angles exist if $v_0 \geq v_0^{cr}$, which defines the instability threshold. When $v_0 = v_0^{cr}$, we have $\varphi = \varphi_{\max}$ with [cf. *Pokhotelov et al.*, 2000]

$$\varphi_{\max} \simeq \pm\pi + \arctan\frac{\alpha_P}{\alpha_H}. \tag{46}$$

Substituting $\varphi = \varphi_{\max} + \Delta\varphi$ into equation (41) and using the expansion $\cos\Delta\varphi \simeq 1 - (\Delta\varphi)^2/2$, one finally obtains the expression for the instability growth rate

$$\gamma = \frac{\pi\alpha_P\alpha_C k_\perp L v_0}{2\alpha_I v_{AI}}\left[1-\frac{v^{cr}}{v_0}-\frac{(\Delta\varphi)^2}{2}\right]. \tag{47}$$

Considering $v_0 \simeq v_0^{cr}$, from (47) for the marginal instability we have

$$\gamma = \left(\frac{\pi}{2}\right)^2\alpha_P\left[1+\frac{\nu}{\alpha_P}\left(\frac{2}{\pi}\right)^2\right]\left[1-\frac{v^{cr}}{v_0}-\frac{(\Delta\varphi)^2}{2}\right]. \tag{48}$$

The growing waves propagate in the cone defined by

$$\varphi_{\max}-[2(1-v^{cr}/v_0)]^{1/2} < \varphi < \varphi_{\max}+[2(1-v^{cr}/v_0)]^{1/2}, \tag{49}$$

and centered around $\varphi_{\max}$.

This scenario is similar to the Čerenkov radiation in collisionless plasma [cf. *Pokhotelov et al.*, 2000]. For the marginal instability ($v_0 \simeq v_0^{cr}$) the growing waves propagate at an angle $\varphi = \varphi_{\max}$ defined by (46).

For $v_{AI} = 500$ km/s and $L = 1000$ km a typical dimensionless recombination frequency is of the order of 5×10^{-3} and the nighttime conductivity $\alpha_P \simeq 0.1$ [e.g., *Lysak*, 1991]. Thus $\nu \ll \alpha_P \ll 1$ and the recombination processes do not suppress the instability during the night. Substituting $\alpha_I = 10^{-1} \div 10^{-2}$ and $\alpha_C \simeq 0.2$ into (45) we estimate the critical velocity as $v^{cr} \simeq 1.25 \times (10^{-2} \div 10^{-1})(\lambda_\perp/L)v_{AI}$. For $\lambda_\perp \simeq 10$ km, $L \simeq 1000$ km and $v_{AI} = 500$ km/s this gives $v^{cr} \simeq (60 \div 600)$ m/s. For $B = 0.5$ gauss this corresponds to the convection electric field of the order of $3 \div 30$ mV/m, which is typical for the polar ionosphere.

5. Discussion and Conclusions

It is shown that the IAR and the feedback instability can be qualitatively described in the framework of a simplified model in which the Alfvén velocity undergoes a final jump at the upper boundary. The only difference with the *Lysak* [1991] model, which uses a smooth exospheric profile of the Alfvén velocity, arises in the values of the IAR eigenfrequencies. However, our model allows us to provide a deeper insight into the physics of this phenomenon. In particular, it was demonstrated that Hall dispersion plays a key role in the IAR damping when Pedersen conductivity approaches the "IAR wave conductivity." The inclusion of this effect into consideration removes inconsistency of the model related to infinite damping at $\alpha_P = 1$. The damping rate becomes dependent on the wavelength and scales as $\propto \ln(\kappa k_\perp L)$ in this region. The cornerstone of our analysis is that a new IAR instability with the lowest threshold has been revealed which was not studied in the course of the earlier analysis.

It is worth mentioning that the IAR instability at $\eta = \pi/2$ in the low conductive ionosphere directly follows from the model which uses a smooth profile of the Alfvén velocity. Let us show that a similar solution for the feedback instability exists in the *Lysak* [1991] basic equation. For simplicity, let us neglect the corrections due to recombination and leakage out of the resonator upper boundary and consider $\nu = \varepsilon = 0$. Note that these effects should just provide the damping. Then from *Lysak* [1991] we get

$$\left(1-\frac{\sigma_\varphi}{x_0}\right)\frac{J_1(x_0)}{J_0(x_0)} = -i\alpha_P. \tag{50}$$

In the low conductivity limit, that is, when $\alpha_P \ll 1$, this equation yields two solutions. The first one corresponds to the case when solution to this equation is close to the roots of the Bessel function of the first order, i.e., when $J_1(\eta_{1m}) = 0$. These roots are related to the eigenmodes of the undisturbed resonator in the limit of low ionospheric conductivity. The lowest nonzero root is equal to $\eta_{10} = 3.8$, which in our model corresponds to $\eta = \pi$. The instability growth rate in this case was evaluated by *Lysak* [1991] and reads

$$\gamma_L = 2^{-1/2}(\alpha_P\eta_{10})^{1/2}. \tag{51}$$

The necessary threshold velocity for the instability onset was given by *Pokhotelov et al.* [2000] and assumes the form

$$v^{cr} = \frac{\alpha_I v_{AI}\eta_{10}}{k_\perp L\alpha_C}. \tag{52}$$

However, as it was shown above, equation (50) yields another solution localized in the vicinity of roots of the zero-order Bessel function, that is, when $J_0(x_0) \simeq 0$ and $\sigma_\varphi \simeq \eta_{0m}$. This is related to the IAR eigenmodes influenced by the presence of convective flow. The lowest instability threshold corresponds to $\eta_{00} = 2.4$. We recall that in a simplified model adopted in our study this root is $\pi/2$ (see Figure 4). Similar to section 4, the expansion of (50) gives

$$(x_0 - \eta_{00})(1 - i\alpha_P\eta_{00}) - (\sigma_\varphi - \eta_{00}) = 0, \tag{53}$$

from which one readily obtains

$$\gamma_P = \alpha_P \eta_{00}^2 \left[1 - \frac{v^{cr}}{v_0} - \frac{(\Delta\varphi)^2}{2}\right], \qquad (54)$$

with

$$v^{cr} = \frac{\alpha_I v_{AI} \eta_{00}}{k_\perp L \alpha_C}. \qquad (55)$$

Expressions (54) and (55) are identical to (48) and (45) if one replaces η_{00} by $\pi/2$ and neglects the recombination frequency ν. Let us compare the values of instability growth rates near $\eta \simeq \eta_{10} = 3.8$ and $\eta = 2.4$. According to (51) and (54) this ratio is

$$\frac{\gamma_L}{\gamma_P} \simeq 0.2\alpha_P^{-1/2}. \qquad (56)$$

For typical nighttime Pedersen conductivity $\alpha_P \simeq 0.1$ both these instabilities have the same order of value, i.e., $\gamma_L \simeq \gamma_P$. With the increase in the ionospheric conductivity the instability growth rates increase. Figure 6 shows the dependence of the instability growth rate as the function of α_P in the vicinity of $\sigma \simeq \pi/2$. It is clearly seen that it approaches the maximum value at low but finite ionospheric conductivity. From comparison of expressions (50) and (53) we conclude that instability threshold at the frequency $\eta \simeq \eta_{00}$ is 1.6 times lower than that at $\eta \simeq \eta_{10}$. Therefore it is reasonable to assume that this instability can be considered the most probable candidate for the IAR excitation.

Thus our analysis shows that the most favorable conditions are realized when the ionospheric conductivity is low. We note that this occurs basically during the nighttime conditions. In this case the dissipation is small, and the electric field of magnetospheric convection can easily penetrate the conductive slab. In such conditions the convection flow moves relatively freely through the ionosphere, losing its energy basically due to Čerenkov radiation in the IAR. These results agree with *Newell et al.* [1996] analysis of data collected from the DMSP satellite showing that the most intense auroral arcs (discrete aurora), which are usually attributed to small-scale Alfvénic structures [e.g., *Stasiewicz et al.*, 2000], appear preferentially in the weakly conducting ionosphere when strong electron precipitation is observed.

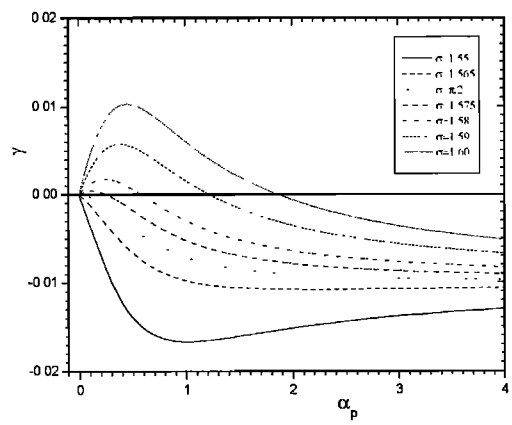


Figure 6. Variation of the growth rate of the fundamental mode in the vicinity of $\eta \simeq \pi/2$. Other parameters are the same as in Figures 4 and 5.

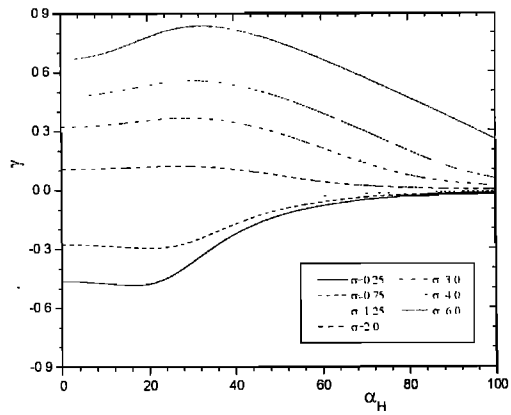


Figure 7. Variation of the IAR damping/growth rate as the function of α_H for different values of σ. Here $\alpha_P = 2$, while other parameters are the same as in Figures 2-6.

In section 4, for simplicity, we have neglected the corrections due to Hall dispersion effects which do not substantially modify the values of the damping/growth rates. However, as was mentioned by *Yoshikawa and Itonaga* [1996], their contribution becomes nonvanishing for rather large values of α_H at fixed α_P. Figure 7 represents an example of the variation of the instability damping/growth rate as a function of α_H in the presence of Hall dispersion effects. One can see that these effects may lead to the appearance of a maximum when the ratio α_H/α_P is sufficiently large. Moreover, the inclusion of this effect into consideration is clearly important for the ground observations, since the direct magnetic signatures of the Pedersen and field-aligned current structures tend to cancel one another [e.g., *Lysak*, 1999].

An important effect that was not considered in our analysis refers to the electromagnetic stratification of the magnetospheric convection that arises as the result of the feedback instability. The detailed scenario of such process has been described by *Trakhtengertz and Feldstein* [1981, 1984, 1987]. Moreover, the relevant nonlinear effects involved in the subsequent evolution of the instability would lead to the formation of a turbulent Alfvén boundary layer (TABL) and appearance of the anomalous conductivity in the IAR region [*Trakhtengertz and Feldstein*, 1984, 1991]. However, the description of these effects is out of the scope of the present study. We should only mention that basic dispersion equation (50) for the IAR eigenmodes yields an additional unstable mode. It starts to grow at the value of the convection velocity defined by expression (55), i.e., at the value of the convection electric field which is 1.6 lower than that predicted by the previous analysis.

Thus the formation of TABL and associated phenomena arise at more moderate ionospheric conditions.

The intention of the present approach is to provide deeper insight into the physics of the IAR and the feedback instability. Hence this paper can be considered as an extension of our previous approach to the study of the IAR [*Pokhotelov et al.*, 2000], which was bounded by consideration of low and high ionospheric conductivity. The results of our study might be useful for a better understanding of the IAR properties, as well as for the interpretation of recent satellite observations by Freja and Fast satellites [e.g., *Stasiewicz and Potemra*, 1998; *Ergun et al.*, 1998; *Stasiewicz et al.*, 2000; *Grzesiak*, 2000].

Acknowledgments. We are grateful to Kalevi Mursula, Jorma Kangas, and Tillman Bösinger for fruitful discussions. One of the authors (O.A.P.) is grateful to R. Z. Sagdeev for valuable comments. The authors acknowledge financial support from the Commission of the European Union (grants INTAS-96-2064 and INTAS-99-0335). O.A.P. acknowledges support from ISTC through research grant 1121-98 and wishes to thank the French Ministère de la Recherche et de la Technologie for hospitality at LPCE, where this work was completed. V.P.P. acknowledges support from the Swedish Natural Science Research Council (NFR) through grant F 809/1999.

Janet G. Luhmann thanks Akimasa Yoshikawa and another referee for their assistance in evaluating this paper.

References

Belyaev, P. P., S. V. Polyakov, V. O. Rapoport, and V. Y. Trakhtengertz, Discovery of the resonance spectrum structure of atmospheric electromagnetic noise background in the range of short-period geomagnetic pulsations, *Dokl. Akad. Nauk SSSR, 297*, 840, 1987.

Belyaev, P. P., S. V. Polyakov, V. O. Rapoport, and V. Y. Trakhtengertz, The ionospheric Alfvén resonator, *J. Atmos. Terr. Phys., 52*, 781, 1990.

Belyaev, P. P., T. Bösinger, S. V. Isaev, and J. Kangas, First evidence at high latitudes for the ionospheric Alfvén resonator, *J. Geophys. Res., 104*, 4305, 1999.

Blagoveshchenskaya, N. F., V. A. Kornienko, T. D. Borisova, B. Thide, M. J. Kosch, M. T. Rietveld, E. V. Mishin, R. Y. Luk'yanova, and O. A. Troshichev, Ionospheric HF pump wave triggering of local auroral activation, *J. Geophys. Res.*, (in press), 2001.

Brekke, A., J. R. Doupnik, and P. M. Banks, Incoherent scatter measurements of *E* region conductivities and currents in the auroral zone, *J. Geophys. Res., 79*, 3773, 1974.

Buchert, S. C., and F. Budnik, Field-aligned current distributions generated by a divergent Hall current, *Geophys. Res. Lett., 24*, 297, 1997.

Ergun, R. E., et al., Fast satellite observations of electric field structures in auroral zone, *Geophys. Res. Lett., 25*, 2025, 1998.

Fraser-Smith, A. C., ULF magnetic fields generated by electrical storms and their significance to geomagnetic pulsation generation, *Geophys. Res. Lett., 20*, 467, 1993.

Greifinger, C., and P. S. Greifinger, Theory of hydromagnetic propagation in the ionospheric waveguide, *J. Geophys. Res., 73*, 7473, 1968.

Grzesiak, M., Ionospheric Alfvén resonator as seen by Freja satellite, *Geophys. Res. Lett., 27*, 923, 2000.

Lysak, R. L., Coupling of the dynamic ionosphere to auroral flux tubes, *J. Geophys. Res., 91*, 7047, 1986.

Lysak, R. L., Theory of auroral zone PiB pulsation spectra, *J. Geophys. Res., 93*, 5942, 1988.

Lysak, R. L., Feedback instability of the ionospheric resonant cavity, *J. Geophys. Res., 96*, 1553, 1991.

Lysak, R. L., Generalized model of the ionospheric Alfvén resonator, in *Auroral Plasma Dynamics, Geophys. Monogr. Ser.*, vol. 80., edited by R. L. Lysak, p. 121, AGU, Washington, D. C., 1993.

Lysak, R. L., Propagation of Alfvén waves through the ionosphere: Dependence on ionospheric parameters, *J. Geophys. Res., 104*, 10,017, 1999.

Mallinckrodt, A. J., and C. W. Carlson, Relations between transverse electric fields and field-aligned currents, *J. Geophys. Res., 83*, 1426, 1978.

Miura, A., S. Ohtsuka, and T. Tamao, Coupling instability of the shear Alfvén wave in the magnetosphere with the ionospheric ion drift wave, 2, Numerical analysis, *J. Geophys. Res., 87*, 843, 1982.

Newell, P.T., C.-I. Meng, and K. M. Lyons, Suppression of discrete aurora by sunlight, *Nature, 381*, 766, 1996.

Newton, R. S., D. J. Southwood, and W. J. Hughes, Damping of geomagnetic pulsations by the ionosphere, *Planet. Space Sci., 26*, 201, 1978.

Pokhotelov, O. A., D. Pokhotelov, A. Streltsov, V. Khruschev, and M. Parrot, Dispersive ionospheric resonator, *J. Geophys. Res., 105*, 7737, 2000.

Polyakov, S. V., and V. O. Rapoport, The ionospheric Alfvén resonator, *Geomagn. Aeron., 21*, 816, 1981.

Rothwell, P. L., M. B. Silevitch, and L. P. Block, A model for propagation of the westward traveling surge, *J. Geophys. Res., 89*, 8941, 1984.

Spiro, R. W., P. H. Reiff, and L. J. Maher, Precipitating electron energy flux and auroral zone conductances: An empirical model, *J. Geophys. Res.*, 87, 8215, 1982.

Stasiewicz, K., and T. Potemra, Multiscale current structures observed by Freja, *J. Geophys. Res., 103*, 4315, 1998.

Stasiewicz, K., et al., Small scale Alfvénic structure in the aurora, *Space Sci. Rev., 92*, 423, 2000.

Sukhorukov, A. I., and P. Stubbe, Excitation of the ionospheric resonator by strong lightning discharges, *Geophys. Res. Lett.*, 24, 829, 1997.

Trakhtengertz, V. Y., and A. Y. Feldstein, Effect of the nonuniform Alfvén velocity profile on stratification of magnetospheric convection, *Geomagn. Aeron., 21*, 711, 1981.

Trakhtengertz, V. Y., and A. Y. Feldstein, Quiet auroral arcs: Ionosphere effect of magnetospheric convection stratification, *Planet. Space Sci., 32*, 127, 1984.

Trakhtengertz, V. Y., and A. Y. Feldstein, About excitation of small-scale electromagnetic perturbations in ionospheric Alfvén resonator, *Geomagn. Aeron., 27*, 315, 1987.

Trakhtengertz, V. Y., and A. Y. Feldstein, Turbulent Alfvén boundary layer in the polar ionosphere, 1, Excitation conditions and energetics, *J. Geophys. Res., 96*, 19,363, 1991.

Trakhtengertz, V. Y., P. P. Belyaev, S. V. Polyakov, A. G. Demekhov, and T. Bösinger, Excitation of Alfvén waves and vortices in the ionospheric Alfvén resonator by modulated powerful radio waves, *J. Atmos. Sol. Terr. Phys., 62*, 267, 2000.

Yoshikawa, A., and M. Itonaga, Reflection of shear Alfvén waves at the ionosphere and the divergent Hall current, *Geophys. Res. Lett., 23*, 101, 1996.

Yoshikawa, A., and M. Itonaga, The nature of reflection and mode conversion of MHD waves in the inductive ionosphere: Multistep mode conversion between divergent and rotational electric fields, *J. Geophys. Res., 105*, 10,565, 2000.

Yoshikawa, A., M. Itonaga, S. Fujita, H. Nakata, and K. Yumoto, Eigenmode analysis of field line oscillations interacting with the ionosphere-atmosphere-solid earth electromagnetic coupled system, *J. Geophys. Res., 104*, 28,437, 1999.

V. Khruschev, O. A. Pokhotelov, S. Senchenkov, Institute of Physics of the Earth, Bolshaya Gruzinskaya, 10, 123 810 Moscow, Russia. (khru@uipe-ras.scgis.ru; pokh@uipe-ras.scgis.ru; liper@uipe-ras.scgis.ru)

M. Parrot, Laboratoire de Physique et Chimie de l'Environnement, Centre National de la Recherche Scientifique, 3A, Avenue de la Recherche Scientifique, F-45071 Orléans, France. (mparrot@odyssee.cnrs-orleans.fr)

V. P. Pavlenko, Department of Space and Plasma Physics, Uppsala University, S-75591 Uppsala, Sweden. (vladimir.pavlenko@rymdfysik.uu.se)

(Received December 6, 2000; revised May 7, 2001; accepted May 7, 2001.)